Decomposition strategy for districts as renewable energy hubs

Luise Middelhauve, Cédric Terrier, and François Maréchal,

In light of the energy transition, it becomes a widespread solution to decentralize and to decarbonize energy systems. However, limited transformer capacities are a hurdle for large-scale integration of solar energy in the electricity grid. The aim of this paper is to define a novel concept of renewable energy hubs and to optimize its design strategy at the district scale in an appropriate computational time. To overcome runtime issues, the Dantzig–Wolfe decomposition method is applied to a mixed-integer linear programming framework of the renewable energy hub. Distributed energy units as well as centralized district units are considered. In addition, a method to perform multi-objective optimization as well as respecting district grid constraints in the decomposition algorithm is presented. The decomposed formulation leads to a convergence below 20 min for 31 buildings and a mip gap lower than 0.2%. The centralized design enhances the photovoltaic penetration in the energy mix and reduces the global warming potential and necessary curtailment in order to respect transformer capacity constraints.

***Index Terms*—Renewable energy hub, decomposition, solar energy integration, district energy system, multi–objective optimization, transformer capacity**

ACRONYMS

ADMM alternating direction method of multipliers; AR annual revenues; BES building energy system; CAPEX capital expenses; DWD Dantzig-Wolfe decomposition; GU grid usage; GWP global warming potential; KPI key performance indicator; MILP mixed-integer linear programming; MOO multi-objective optimization; MP master problem; OPEX operational expenses; PV photovoltaic; PVC PV curtailment; PVP PV penetration; SC self-consumption; SP subproblem; SS self-sufficiency; TOTEX total expenses

I. INTRODUCTION

The electrification of the building sector and the simultaneous increase of locally generated electricity from renewable energy sources, is one of the most promising mitigation pathways in the battle of climate change. However, 50% of the global final energy use in residential buildings is related to thermal not electrical end-use [1]. This shows that the plan of decarbonizating the building stock requires a holistic concept, following a multi-energy approach. Additionally, the volatile power generation, which is caused by the fluctuation of solar irradiation, challenges the capacity of the electrical power grid [2]. Therefore, in addition to maximizing the solar integration, it is important to reduce the interaction of building energy systems (BESs) with the electrical power grid. These requirements are fulfilled by the concept of energy hubs. However, the precise definition is difficult to pin-point.

A review with more than 100 contributions in the field of energy hubs has been provided by Mohammadi et al. [3]. The demonstrated consensus was that an energy hub is a place, which has in-flows, out-flows and considers the interconnection of multiple energy carriers. Additionally, the aspect of optimally controlling the operation of an energy hub has been included in most studies. The optimal investment of equipment for the energy hub was in general not considered. Nevertheless, Maroufmashat et al. [4] have considered different pre-defined energy hub scenarios and the interaction between a collection of energy hubs. The result has shown that the importance of the interactions increased with the number of integrated hubs. A maximum of three interconnected energy hubs have been studied by Maroufmashat et al. [4].

Upscaling a collection to contain several interconnected energy hubs is computationally problematic as the runtime increases exponentially with the number of buildings. The goal is to find an algorithm, which can optimize, with sufficient speed and accuracy, the schedule and the design of an energy system considering several dozen buildings. It is indeed an ongoing discussion in the field that researchers seek for the most suitable method to reach this goal. An overview of the state-of-the-art is presented in Table I and further discussed in the following.

TABLE I: Limitation of decomposition approaches.

approach	limitation	source
aggregation	oversimplification, no network interactions	[5]
bi-level	high runtime	[6],[7]
Benders	limited handling of integers in SPs	[8]
ADMM	limited number of SPs, runtime	[9],[10]

One option is the reduction of the spatial resolution using typical buildings as demonstrated by Stadler et al.[5]. Whereas these aggregation methods effectively decrease the computation time, they often oversimplify the problem and render the individual BES design impossible. Therefore, this approach is not suitable for distributed energy systems that require a low level of detail. Decomposition methods are seen as the best candidates to handle the increasing complexity of energy system models. A good overview about mathematical decomposition methods has been provided by Grossmann

This paragraph of the first footnote will contain the date on which you submitted your paper for review. It will also contain support information, including sponsor and financial support acknowledgment. For example, "This work was supported in part by the U.S. Department of Commerce under Grant BS123456".

L. Middelhauve C. Terrier and F. Maréchal are with Department for Industrial Processes and Energy Systems Engineering, École Polytechnique Fédérale de Lausanne, Sion, Switzerland. (Corresponding e-mail: luise.middelhauve@epfl.ch)

et al. [11]. The main and most common approaches are bi-level, Benders and Lagrangean decomposition [11]. A popular method to investigate the scheduling and design of energy systems is the bi-level decomposition [6]. The method relies on a heuristic approach and has, therefore, a high computational time. Morvaj et al. [7] have reported a runtime between 12h-30h for an optimization of 5 buildings. In contrast, the Benders and Lagrangean decomposition efficiently decrease the optimization runtime. The difference between the two methods is that the former deals with linking variables and the latter deals with linking constraints. These linking terms are the main reason for the optimization to become computationally expensive since they are linking several independent problems. The basic principle of these decomposition methods is that the problem is split into a master problem (MP), handling the linking terms, and subproblems (SPs), which are the resulting, independent sub-parts of the original problem. The advantages of the Lagrangean and Benders decomposition are the convergence guarantee, the speed and the ease to scale up the optimization problem with the parallelization of solving the SPs [12]. The drawback of the Benders decomposition is the incapability to handle integer variables in the SPs [8], which are a requirement for taking decisions about the energy system. There are proposed solutions that overcome the issue for a limited number of integers, such as by Fakhi et al. [8], but these remain insufficient for the optimization of district size energy hubs.

The Lagrangean decomposition has been further developed to the alternating direction method of multipliers (ADMM) and Dantzig-Wolfe decomposition (DWD) [13]. The ADMM is an extended version of the augmented Lagrangean method. It handles optimization problems that can be split into two main objective functions. The convergence is guaranteed [14] but only for the limited number of two splits [9]. Additionally, the ADMM is computationally outperformed by the DWD [10].

The DWD algorithm allows individual design and scheduling of distributed and centralized energy units within entire district energy systems. It overcomes the scalability issue of the ADMM [12] as well as the limitations of presented state-of-the-art methods in Table I. In addition, the algorithm is straightforward to implement as the SPs require minor adaptations during the re-formulation in order to obtain the decomposed problem [15]. Historically the DWD has been designed for linear problems. However, Harb et al. [16] and Schütz et al. [15] have demonstrated how it can be applied to mixed-integer linear programming (MILP) problems. Neither of both studies has considered a multi-objective optimization (MOO) framework in its optimization of energy hubs at the district scale.

Literature in the field of the coordinated design and operational scheduling of energy hubs at the district scale has revealed that the computational effort remains a major hurdle. Even with the great simplification of aggregating down to 4 buildings, the runtime reported by Yang et al. [17] is close to 6 hours. Applying decomposition strategies Wakui et al. [18] have reported a runtime between 2-55.5 hours for a single optimization of 5-100 buildings. Schütz et al. have required [15] 2.6 hours for an optimization of 10 buildings. Reviewed studies have often oversimplified the model considering only the grid operation or the electricity layer [3].

Based on the main findings reported in the aforementioned literature review, this work contributes to the following research topics:

- How can an optimization framework of an entire district be solved in acceptable runtime and accuracy using the DWD? How can multi-objective optimization be applied to the DWD?
- What is the benefit of a community-based design and operation of energy hubs? Thereby, including the following aspects:
  - investment decisions for central and distributed energy units;
  - multi-energy systems, integrating not only electrical but also thermal energy demands;
  - interactions of distributed energy systems within the community for both the optimal design as well as optimal scheduling;
  - the potential of synergies within distributed renewable energy hubs with respect to grid-aware design and to overcome limitations imposed by the power grid;

II. Materials and methods

A. Overview of the compact MILP formulation

The novelty of this work is based on the concept of renewable energy hubs at different scales that includes investment decisions. A renewable energy hub is defined as a center of optimally interconnected energy carriers that contains conversion and storage units and maximizes its own usage of renewable energy sources. A renewable energy hub is embedded in a superior network and considered at different scales. The decisive factor is the level at which investment decisions are made.

The MILP problem formulation of the renewable energy hub is based on the modeling technique of BES by Stadler et al. [5], which was further developed by Middelhauve et al. [19]. Three types of energy demands are considered: space heating, domestic hot water and electricity. Each BES is connected to utility grids (natural gas, fresh water and electricity) and contains energy conversion and storage units. A smart space heating management is considered based on a thermal 1R1C model of the buildings. Optimal scheduling is included while respecting energy and resource balances as well as the heat cascade. The main decision variables are the decision to install a unit (binary variables), the size of the unit in case it is installed (continuous variables) and the orientation of photovoltaic (PV) modules. Space heating and domestic hot water demands can be supplied by a gas boiler, an air-water heat pump or two electrical heaters and two thermal storage tanks, one for each thermal demand.

Electricity can be generated by PV panels, which can be mounted on the roofs and facades of buildings, and stored in lithium batteries. Annual time series are aggregated to typical and extreme operating periods with the K-medoids clustering algorithm. Daily cyclic constraints are applied to the storage technologies. In the following the main modeling equations are outlined based on four main sets, which are the unit U, the typical period P, the timestep of the typical period T and the building B.

As the scale of the renewable energy hub is defined by the level at which the investment decisions are taken, there are two different scales considered in this work: the building and the district scale. If the investment decisions are taken from the perspective of the building's owner, the energy hub is at the building scale. In case the investment decisions are taken from the perspective of the community, the renewable energy hub is considered at the district scale. Therefore, a district can either be considered as a collection of energy hubs at the building scale or as one energy hub at the district scale. The former corresponds to a decentralized design strategy, the latter to a centralized one. Since a compact formulation of the centralized strategy is computationally infeasible, the model is decomposed.

B. General structure of the decomposition

Similar to other decomposition strategies, the problem is split into a MP and several SPs, when performing the DWD. The MP is a reformulation of the original problem, whereas the SPs are independent parts within the original problem. The SPs are usually linked to the overall problem with only a few constraints. Thus, independent subblocks and their linking constraints need to be identified in the compact formulation in a first step. In the case of district energy systems, it translates into building energy systems as subblocks and network balances as their linking constraints (Figure 1). In a second step, the SPs are substituted in the MP by a linear combination of their extreme points. The Minkowski's representation theorem states that a bounded problem is identical when only described with its extreme points [12]. In the DWD method, this behavior is exploited for moving most of the constraints to the SPs, leaving only the linking constraints and the linear combination of extreme points in the MP. For the application to district energy systems, this translates into the network model as MP, which considers different optimal solutions from the SPs (Figure 1). The connection of the MP to the SPs is established in two ways: the SPs send their optimal design proposals to the MP, whereas the MP sends price signals to the SPs. The price signals represent incentives to change the design of the SPs in order to improve the overall objective of the district.

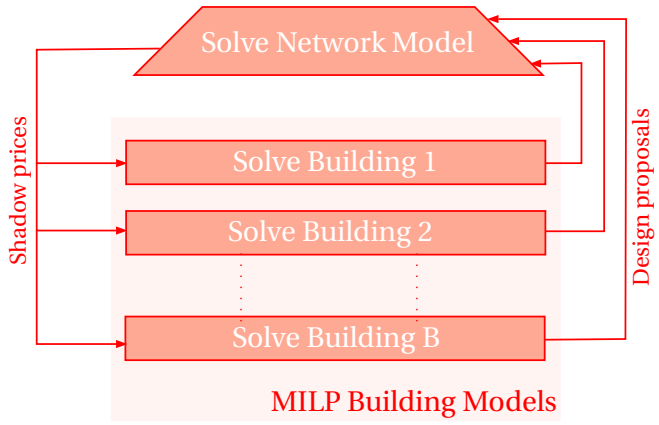

Fig. 1: Application of the DWD principle [10] to the design and operation optimization of centralized energy systems.

The application of the DWD algorithm to the framework of renewable energy hubs is summarized in Table II. The SPs correspond to individual BESs and the MP to the district model. The latter considers all network constraints, such as the electricity balance at the transformer and electricity exchanges within the district.

TABLE II: DWD Algorithm and the corresponding part in the decomposition of renewable energy hubs at the district scale. Interpretation of dual values depends on the corresponding constraints.

Dantzig–Wolfe algorithm	**application renewable energy hubs**
master problem (MP)	district model
linking constraints	network constraints
independent subproblems (SPs)	building energy system (BES) models
solution candidates	design proposal BES
dual values of linking constraints	f.e. microgrid tariff

The advantage of this method is that it exploits the natural structure of a district energy system and single buildings can be included with their own characteristics. Furthermore, this structure conveniently allows for using the decentralized approach, which is detailed in [19]. Only the objective functions have to be adjusted in order to formulate the SPs.

C. Master problem

The MP consists of all aspects which are linking the SPs. Thus, in the application of centralized planning of renewable energy hubs, the MP contains all network-related equations, such as the electricity grid, and centralized units or constraints. The overall aim of the MP is to coordinate operation and design proposals within the district and to minimize exchanges to/from the district. The design proposals include the investment decisions of technologies, the natural gas costs and the exchange schedule of the SPs within the district network.

In the following, the MP is detailed. The main sets remain unchanged, the additional set I keeps track of all iterations of the algorithm. Dual variables are linked to their specific equation with the expression $\backsim$ [ ] and addressed at a later point in this section. Variables are specified with ***bold*** characters.

$$0 \leq \boldsymbol{\lambda_{i,b}} \leq 1 \quad \forall i \in \mathrm{I}, \quad \forall b \in \mathrm{B} \tag{1a}$$

$$\sum_{i \in \mathrm{I}} \boldsymbol{\lambda_{i,b}} = 1 \quad \forall b \in \mathrm{B} \quad \backsim [\mu_b] \tag{1b}$$

The new decision variable of the MP is λ, which decides for ($\lambda = 1$) or against ($\lambda = 0$) proposals. The optimal solution is a linear combination of these points [12]. Convexity Equations 1a and 1b ensure that a proposal can be chosen maximal once and that the linear combination of all selected proposals does not exceed one. The dual variable associated to (1b) is μ.

$$\sum_{i \in \mathrm{I}} \sum_{b \in \mathrm{B}} \boldsymbol{\lambda_{i,b}} \cdot \left(\dot{E}^{gr,+}_{i,b,p,t} - \dot{E}^{gr,-}_{i,b,p,t} \right) \cdot d_p \cdot d_t = \boldsymbol{E^{tr,+}_{p,t}} - \boldsymbol{E^{tr,-}_{p,t}}$$
$$\forall p \in \mathrm{P}, \quad \forall t \in \mathrm{T} \quad \backsim [\pi_{p,t}] \tag{2}$$

The main linking constraint is the electricity balance at the transformer tr of the district (2). The MP receives the grid exchange $E^{gr,\pm}$ from each building b in each iteration i, and balances the load on the transformer level. The associated dual variable of the network constraint is π. Since the frequency d_p of the period and the timestep duration d_t are considered in (2), π and $E^{tr,\pm}$ are evaluated with their annual impact.

$$\boldsymbol{C^{el}} = \sum_{p \in \mathrm{P}} \sum_{t \in \mathrm{T}} \left(c^{el,+}_{p,t} \cdot \boldsymbol{E^{tr,+}_{p,t}} - c^{el,-}_{p,t} \cdot \boldsymbol{E^{tr,-}_{p,t}} \right) \tag{3}$$

The annual cost for electricity C^{el} of the district is calculated in Equation (3). The cost is based on the total electricity purchase of the system $E^{tr,+}$ and the purchase price $c^{el,+}$ as well as the feed-in revenues $c^{el,-} \cdot E^{tr,-}$.

$$\boldsymbol{C^{op}} = \boldsymbol{C^{el}} + \sum_{i \in \mathrm{I}} \sum_{b \in \mathrm{B}} \boldsymbol{\lambda_{i,b}} \cdot C^{gas}_{i,b} \tag{4a}$$

$$\boldsymbol{C^{cap}} = \sum_{i \in \mathrm{I}} \sum_{b \in \mathrm{B}} \boldsymbol{\lambda_{i,b}} \cdot C^{cap}_{i,b} \tag{4b}$$

$$\boldsymbol{C^{tot}} = \boldsymbol{C^{cap}} + \boldsymbol{C^{op}} \tag{4c}$$

The implemented objectives of the MP are presented in (4a-4c). Objectives can be the operational expenses (OPEX) (4a), the capital expenses (CAPEX) (4b) or the total expenses (TOTEX) (4c). Input parameters coming from the design proposals of the SPs are the capital costs of each BES (C^{cap}) and the operational expenses connected to the purchase of natural gas (C^{gas}).

D. Dual variables

The dual variables in the DWD are used as communication between the MP and the SPs. They signal each SP how the overall objective value of the MP would improve if they change their contribution to a specific linking constraint.

$$[\mu_b] = \frac{\Delta \mathrm{obj}}{\Delta \left(\sum_{i \in \mathrm{I}} \boldsymbol{\lambda_{i,b}} \right)} \quad \forall b \in \mathrm{B} \tag{5}$$

The dual variable $[\mu]$ is associated to (1b) and has the same physical unit as the objective function. As (1b) is defined for each building b, it translates to a dual variable which is specific to each building b and indicates how the network objective value changes if the SP modifies its design proposal (5).

$$[\pi_{p,t}] = \frac{\Delta \mathrm{obj}}{\Delta \left(\boldsymbol{E^{tr,+}_{p,t}} - \boldsymbol{E^{tr,-}_{p,t}} \right)} \quad \forall p \in \mathrm{P}, \quad \forall t \in \mathrm{T} \tag{6}$$

The dual variable $[\pi]$ in (6) is related to the electricity balance at the transformer (2). It indicates how much the overall objective function changes if the electricity exchange at the transformer varies at the timestep t in period p. If the objective function of the MP is the OPEX, the variable $[\pi]$ can be interpreted as electricity price (currency / kWh) within the community. In this case, the lower bound of $[\pi]$ is the feed-in tariff and the upper bound is the retail tariff. For example, in times of net import at the transformer, the district purchases additional electricity at the retail tariff. In contrast, if a building is consuming less electricity, it would overall save the amount corresponding to the retail tariff.

E. Subproblem

One major advantage of the DWD is that the decentralized MILP formulation can be used, with an adjustment of the objective functions, to formulate the SPs. The basis of the BES is described in [5], individual orientation of the roof surfaces are detailed in [20] and shadow casting among buildings and solar integration is considered according to [19]. In the following, the modified objective functions are detailed.

$$\mathrm{obj}_b = \min(\boldsymbol{C^{op}_b} - \mu_b) \quad \forall b \in \mathrm{B} \tag{7a}$$

$$\boldsymbol{C^{op}_b} = \sum_{p \in \mathrm{P}} \sum_{t \in \mathrm{T}} \Big(\pi_{p,t} \cdot \boldsymbol{\dot{E}^{gr,+}_{b,p,t}} - \pi_{p,t} \cdot \boldsymbol{\dot{E}^{gr,-}_{b,p,t}} + c^{ng,+}_{p,t} \cdot \boldsymbol{\dot{H}^{gr,+}_{b,p,t}} \Big) \cdot d_t \cdot d_p \quad \forall b \in \mathrm{B} \tag{7b}$$

The dual variable $[\pi]$ replaces the electricity tariffs in the calculation of operational costs C^{op} (7b). The objective function for each SP (7a) is the modified OPEX subtracted with the dual variable $[\mu]$, which is also called the reduced cost of operation. The SP can still improve the overall objective of the MP if the reduced cost is negative. Whereas, the SP is not able to propose a solution improving the objective of the MP in case of a positive value [12].

$$\mathrm{obj}_b = \min(\boldsymbol{C^{cap}_b} - \mu_b) \quad \forall b \in \mathrm{B} \tag{8}$$

The reduced cost of investment are formulated with the dual variable $[\mu]$, in order to minimize capital expenses C^{cap}. The capital expenses calculation of a single BES is detailed in [21]. As the linking constraint of the electricity grid plays no role in a problem with (8) as objective, the reduced cost of investment is independent from the dual variable $[\pi]$.

$$\mathrm{obj}_b = \min(\boldsymbol{C^{op}_b} + \boldsymbol{C^{cap}_b} - \mu_b) \quad \forall b \in \mathrm{B} \tag{9}$$

The reduced cost of total expenses is detailed in (9). The incentive to change the operation schedule is accounted for with the dual variable $[\pi]$ in the operational costs C^{op}, which are calculated according to (7b).

F. Transformer constraint

The centralized design strategy enables the usage of centralized constraints and limitations, such as the maximum capacity of the local low-voltage transformer (10a). Since the transformer constraint is a linking constraint, it is included in the MP. Additional dual variables are not necessary as the dual variable $[\pi]$ accounts for this limitation. In order to send feasible design proposals to the MP, the SPs are initialized with the equivalent grid usage (GU) (10b, 10c). The GU is the ratio of the transformer capacity to the maximum uncontrollable load of the buildings $\dot{E}^{bui,-}$ [22]. These constraints (10b, 10c) are only required during the initiation of the algorithm and are removed during the iterative process.

$$\dot{\boldsymbol{E}}^{\boldsymbol{tr},\pm}_{\boldsymbol{p,t}} \leq \dot{E}^{tr,max} \quad \forall p \in \mathrm{P}, \quad \forall t \in \mathrm{T} \tag{10a}$$

$$\mathrm{GU}^{\pm} = \dot{E}^{tr,max} / \max_{p,t}(\sum_{b \in B} \dot{E}^{bui,-}_{b,p,t}) \tag{10b}$$

$$\dot{\boldsymbol{E}}^{\boldsymbol{gr},\pm}_{\boldsymbol{b,p,t}} \leq \mathrm{GU}^{\pm} \cdot \max_{p,t}(\dot{E}^{bui,-}_{b,p,t}) \quad \forall b,p,t \in \mathrm{B,P,T} \tag{10c}$$

G. Multi-objective optimization

Multi-objective optimization is in general necessary to detect a selection of optimal solutions for two, or more, conflicting objective functions. These can be used to generate pathways and analyze trade-offs to reach an ultimate goal. In the decentralized approach, the MOO is an algorithm which uses ϵ-constraints to generate a Pareto curve [19]. While the first objective is optimized, ϵ-constraints serve as incrementally increasing upper bounds of the second objective function. Then, the position of the first and second objective is inverted. In the context of the DWD, the ϵ-constraint translates into a linking constraint, which impacts the entire network.

TABLE III: Adjustments for the CAPEX - OPEX MOO using ϵ-constraints. Objective of MP remains unchanged, the ϵ-constraint is added to the MP and its dual variable is included in the objective function of the SPs.

	$\mathbf{Obj}_1$ minimization and $\mathbf{Obj}_2$ constrained
Objective MP	$\min(\boldsymbol{obj_1})$
ϵ-constraint MP	$\boldsymbol{obj_2} \leq \epsilon^{obj_2} \quad \backsim [\beta^{obj_2}]$
Dual variable	$[\beta^{obj_2}] = \Delta \boldsymbol{obj1} / \Delta \epsilon^{obj_2}$
Objective SPs	$\min(\boldsymbol{obj_{1,b}} + \beta^{obj_2} \cdot \boldsymbol{obj_{1,b}} - \mu_b) \quad \forall b \in \mathrm{B}$

Table III provides an overview about the necessary changes for generating the OPEX - CAPEX pareto curve with the DWD. The objective function of the MP needs no adjustments. The ϵ-constraint is added to the MP. Its connected dual variable is $[\beta]$ and it indicates how much the objective of the MP improves in case the respective ϵ limit is relaxed. The dual variable $[\beta]$ is included in the corresponding objective function of the SPs, where it serves as weight between the conflicting objectives.

H. Algorithm

The DWD is an algorithm, where the set of possible solutions in the MP increases with iteration. During the MOO all detected proposals of one Pareto point are kept for the calculation of further points. The algorithm can be separated in four main parts, the initialization, the iteration, the termination and the finalization. Each part is further discussed in the following paragraphs.

a) Initiation: The goal of the initiation is to detect the first values of the dual variables. The dual variable $[\beta]$ is used to initialize 3 different solutions with varying CAPEX-OPEX weights of each SP. In case of a TOTEX single-objective optimization, $[\beta]$ is initialized with the values 0.8, 1 and 1.1. The results are communicated as first design proposals to the MP. In order to initialize the MOO, the dual variable $[\beta]$ is passed with the values 50, 1, and 0.1 to mark the characteristic points of the Pareto curve.

b) Iteration: The iteration process is described in Figure 1. After the first execution of the MP, the dual variables are sent to the SPs as incentive to update their proposals. All SPs are optimized with their modified objective functions (7), (8), (9) or as in Table III. The new design proposals are added to the pool of design proposals of the MP. Afterwards, the relaxed optimization of the MP (continuous λ) is executed and a new set of dual variables are calculated. The iteration continues until a termination criteria is reached.

c) Termination criteria: Four termination criteria are implemented. To check the optimality, the reduced cost of the last optimal proposal of each SP is calculated. If the reduced costs of every SP are greater than or equal to zero, no BESs can improve the overall objective any further by changing their design proposal. Thus, the optimum is found and the algorithm is terminated [12]. Three additional termination criteria are implemented for security reasons: (i) the total CPU time reaches a predefined limit (ii) the total number of iterations reaches a predefined limit (iii) last iterations did not lead to a significant improvement of the overall objective function.

d) Finalization: When one termination criterion is satisfied, the iteration breaks and the algorithm enters its final stage. The MP is executed with binary decision variables $\lambda_i \in \{0;1\}$. This step is necessary to choose discrete integer decisions of the SPs. The integrality constraints are already respected in the SPs, this final step also respects them in the MP [15]. The final decision for a design proposal is returned and the algorithm ends.

I. Key performance indicators

In addition to the objective value, six key performance indicators (KPIs) are used (11a)-(11f). For the sake of readability, the values are expressed in annual terms. The self-consumption (SC) is the share of the onsite generated electricity $E^{site,+}$, that is consumed by the district itself (11a). The self-sufficiency (SS) (11b) is the share of electricity demand, that is covered by onsite generated electricity. The PV penetration (PVP) (11c) measures the amount of onsite generated

electricity with respect to the total electricity demand. The PV curtailment (PVC) (11d) is the share of the onsite generated electricity that is curtailed. The annual revenues (AR) (11e) is the benefit from selling onsite generated electricity to the grid and from avoiding electricity imports. Finally, the global warming potential (GWP) (11f) is the sum of the emissions related to the operation G^{op} (11f) and construction G^{bes} of the BES. A dynamic emission profile is taken for the carbon content of the electricity from the grid. More information on the KPIs calculation is given in previous work [23].

$$\text{SC} = (E^{site,+} - E^{tr,-})/(E^{site,+}) \tag{11a}$$

$$\text{SS} = (E^{site,+} - E^{tr,-})/(E^{site,+} - E^{tr,-} + E^{tr,+}) \tag{11b}$$

$$\text{PVP} = E^{site,gen}/(E^{site,+} - E^{tr,-} + E^{tr,+}) \tag{11c}$$

$$\text{PVC} = (E^{site,gen} - E^{site,+})/E^{site,gen} \tag{11d}$$

$$\text{AR} = (c^{el,+} \cdot SC - c^{el,-} \cdot (1 - SC)) \cdot (E^{site,+}) \tag{11e}$$

$$\text{G}^{op} = \sum_{\substack{p \in P \\ t \in T}} \left(g_{p,t}^{el,TR} \cdot (E^{tr,+} - E^{tr,-}) + \sum_{b \in B} g_{p,t}^{ng} \cdot H_{b,p,t}^{gr,+} \right) \tag{11f}$$

J. Application

The general modeling framework presented in the previous sections A-J is applied to a specific district. The aim of the application is not necessarily to arrive at generally applicable results, but rather to demonstrate the potential of the proposed algorithm and show the benefits of centralized optimization of distributed energy systems. The DWD algorithm was applied to a residential district with a mix of 31 single- and multi-family houses, all connected to the same low-voltage transformer. The district is located in the climatic zone of Geneva, Switzerland. Weather data were clustered into ten typical days. All roof surfaces of the district were integrated with their individual orientation as described in [20]. The sources of the buildings and weather data have been further detailed in [19]. The four termination criteria were set to 1) a maximum of 9 iterations 2) a maximum runtime of 20 minutes 3) an improvement of less than 0.005% during the last 5 iterations and 4) the reduced costs of all SPs greater or equal 0. The problem was formulated in AMPL Version 20210220 and solved with CPLEX 20.1.0.0 on a local machine with the following processor details: Intel(R) Core(TM) i7-9700K CPU @ 3.60 GHz. The relative tolerance between relaxed linear problem and best integer solution was set to *mipgap*=5e-7.

III. Results and Discussion

The goal of the results section is first to validate the decomposition algorithm and second to demonstrate its potential on a real-world application. The validation is carried out by comparing the result of the decomposed optimization to the corresponding result of the compact formulation. These two solving strategies of the same problem should ideally result in the same outcome. The goal of the second part of the results section is to highlight the benefits of considering renewable energy hubs at the district scale. Special focus is given to the grid-aware integration of solar energy. The benefits of coordinated design of distributed energy systems are highlighted by the comparison of the centralized design strategy to the decentralized design strategy, as analyzed in [19] .

A. Convergence and validation

The motivation to use a decomposition algorithm is to ease computational effort while keeping the optimality and accuracy of the solution. The validation of the algorithm was achieved by the comparison to the compact problem. Figure 2 shows the runtime comparison of the compact formulation with the corresponding decomposed problem for the different district sizes. The objective function was TOTEX. The

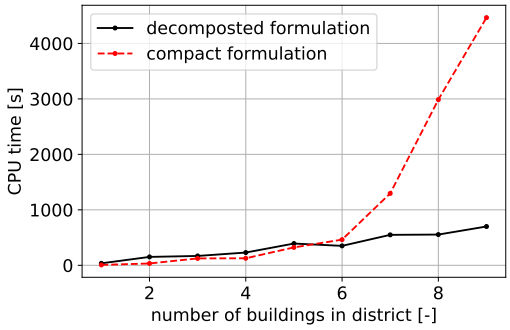

Fig. 2: Comparison of the computational effort with and without decomposition of the problem.

runtime of the compact formulation followed an exponential trend, whereas the effort of the decomposed formulation increased linearly (Figure 2). Minor variations of the CPU time from the linear trend line are explained by the different number of iterations needed to terminate the algorithm. The analysis of an entire low-voltage grid requires the integration of several dozen buildings. Therefore, The optimization of the renewable hub at the district scale is only possible with the decomposed formulation. Figure 3 shows the convergence of the iterative decomposition process. At each iteration, the current objective

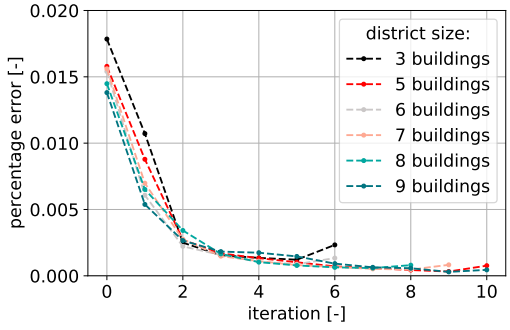

Fig. 3: Convergence of the DWD. Percentage error of the objective function with respect to the corresponding compact model for each iteration.

function was compared to the final objective function of the

corresponding compact formulation (Figure 3). The initialization was already close to the optimum with less than 2% divergence. It can be observed that the bigger the problem size, the smaller was the error in the first iterations. In general, the error dropped below 0.25% already in the first two iterations. The algorithm was terminated after between 5 and 9 iterations. The latter is the maximum of allowed iterations, which was set as termination criterion. In Figure 3, one additional iteration was added for each optimization to visualize the impact of the finalization. During the finalization, the MP is executed one more time with binary instead of continuous variables. This introduced an error that is neglectfully small and decreased with an increase of the problem size. The result of the MOO

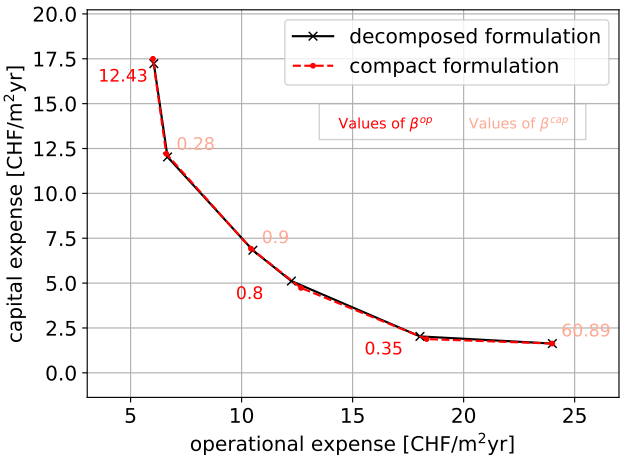

Fig. 4: Validation of the decomposed formulation. CAPEX - OPEX Pareto curve of the MOO for a district size of 11 buildings.

between the CAPEX and the OPEX for a district containing eleven buildings is shown in Figure 4. The decomposition can be validated as also the Pareto frontier was well detected.

B. Benefit of central design strategies

The ongoing discussion in the field of planning and controlling urban energy systems comprises two fundamentally different strategies. Both strategies are mirrored in the two different optimization approaches of the paper. The decentralized optimization considers the renewable energy hub optimal from the perspective of building owners and the centralized optimization from perspective of the entire community. To reach the optimum with a centralized approach it is assumed that a central actor is investing and operating the district. Such actors correspond to distribution system operators, private companies or community associations, whose benefits are the improved operation and investment strategy of the district. The aim of this section is to analyze the magnitude of these benefits.

The result of MOO of both optimization strategies is displayed in Figure 5. The annual OPEX ranged from 31 to 10 CHF/m^2. The minimum CAPEX and the maximum OPEX were the same for both strategies, around 1.4 and 31 CHF per energy reference area, respectively. This is because there are no centralized or interacting units between buildings in the solution with the lowest CAPEX. As a result, the cheapest investment for each building is also the cheapest investment for the community. The centralized strategy remained non-dominated in each scenario along the Pareto curve. Using the centralized strategy, a 5% increase in the CAPEX allowed for a 30% decrease in the OPEX. In contrast, the decentralized design strategy required an increase in the CAPEX by more than 180% (from 1.4 CHF/m^2 to 4 CHF/m^2) for the same reduction in the OPEX. This behavior can be explained in part by how generated electricity is used in both strategies. Initial reductions in the OPEX were characterized by switching from natural gas resources to electricity, followed by the integration of renewable energy sources, and finally by the installation of electricity storage systems (i.e., batteries). The centralized design strategy produced results with a higher share of re-imports. Hence, the centralized strategy allowed an improved coordination of the district. The share of re-imports remained higher for the centralized design strategy, even when electricity production is increased in the district. To decrease the annual OPEX below 12 CHF/m^2, electrical storage systems were used, demonstrating another benefit of the centralized approach: whereas re-import share further decreased to 0 when using the decentralized strategy, the coordinated operation allowed the share of re-imports to be increased to 30%.

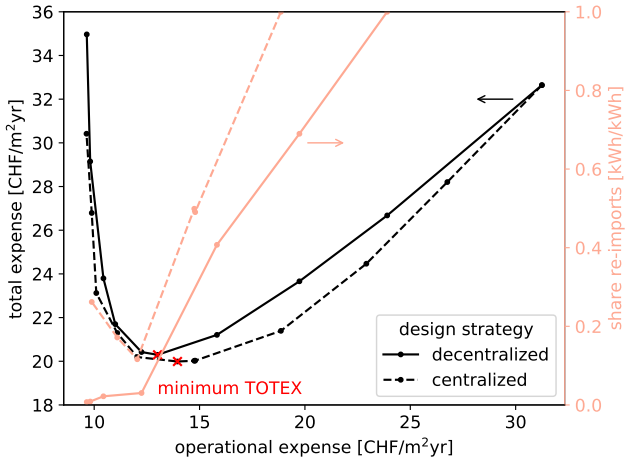

Fig. 5: TOTEX and share of re-imports of generated electricity for increasing OPEX.

In MILP optimization, even a small difference in objective values can lead to very different system configurations. To have a clearer picture of the potential of centralized optimization, a comparison was made with identical objective values. As the centralized optimization was non-dominated along the Pareto frontier, the objective value of the centralized strategy was increased in order to meet the minimum TOTEX of the decentralized strategy.

The KPIs obtained from this analysis are shown in Figure 6. The PVP and SS of the centralized solution was 40% and 20% higher than in the solution identified using the decentralized strategy, respectively. The centralized design strategy of the

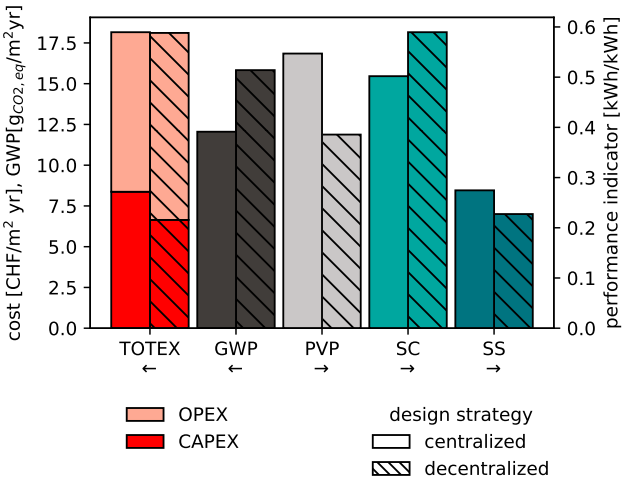

Fig. 6: Comparison of optimal solutions with identical TOTEX for a residential district with 31 buildings.

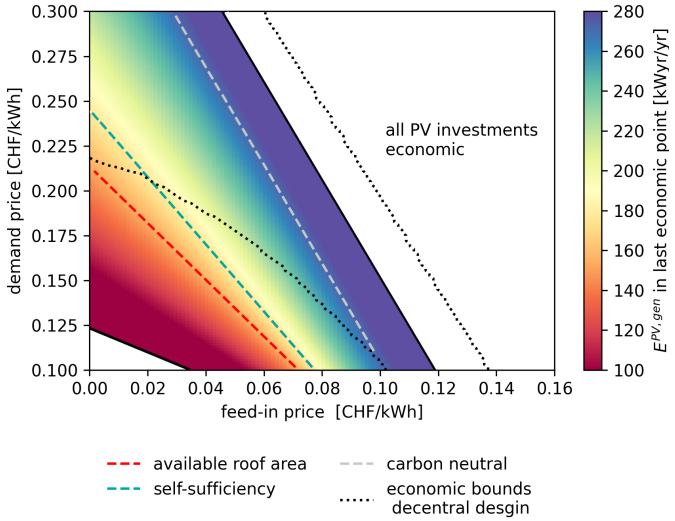

Fig. 7: Variation of the PV yearly generation to achieve break-even as a function of feed-in and demand prices. Point of self-sufficiency with ideal storage, carbon neutrality with life cycle assessment of the equipment and dynamic emission profiles.

distributed energy system allowed a reduction of the GWP of more than 20% for the same TOTEX. The coordinated investment strategy of PV panels and the improved utilization of generated electricity allowed for an electrification of the system without increasing the TOTEX.

With the aim of increasing the share of renewable energy sources, the economically feasible range of solar energy in the district is a matter of interest. From the perspective of the investors, this includes the number of PV panels that can be fully paid back by the end of their lifetime. From the perspective of policymakers, this translates into the question, how to establish energy tariffs to create incentives for a desired PVP in the electricity grid. The cost of PV panels per generated electricity increased with the PV investments. In later investment stages, all profitable surfaces are covered and less profitable surfaces, like north facades, were the only options left. At the same time, the annual revenues decreased with increasing investment into PV panels. The last economically feasible point occurs when the investment cost of the PV panel and their revenues break-even.

This economic analysis was extended to a wide range of tariffs in Figure 7. The analysis shows that PV investments started to be economically feasible at tariffs as low as 0/12 ct/kWh or 3/10 ct/kWh for feed-in and demand price, respectively. At a feed-in price of 12ct/kWh, all PV installations were economically feasible, even at demand price as low as 10 ct/kWh. The economic bounds of the decentralized design strategy are also indicated in Figure 7. The economically feasible region begins at much higher tariffs (10/10 ct/kWh and 0/22 ct/kWh), further demonstrating the benefit of a centralized, coordinated design strategy. Additionally, three points are added in Figure 7, which are the points where the available roof surfaces, self-sufficiency and carbon neutrality are achieved. As the amount of electricity generated was linearly correlated with the electricity tariffs, these points lie along a straight line. To achieve SS with PV panels alone, storage systems are required to balance the mismatch between electricity generation and consumption. The point of SS therefore depends on the round-trip efficiency of these storage systems. The SS was considered with ideal storage systems in Figure 7. More realistic cases of SS lie above the indicated line (8/10 ct/kWh and 0/25 ct/kWh for combination of feed-in/demand price).

Another benefit of the centralized design strategy is the possibility to include centralized requirements that concern the entire system, such as the maximum capacity of the local low–voltage transformer. The load duration curves for different energy system scenarios are shown in Figure 8. The energy system design, which is currently installed in

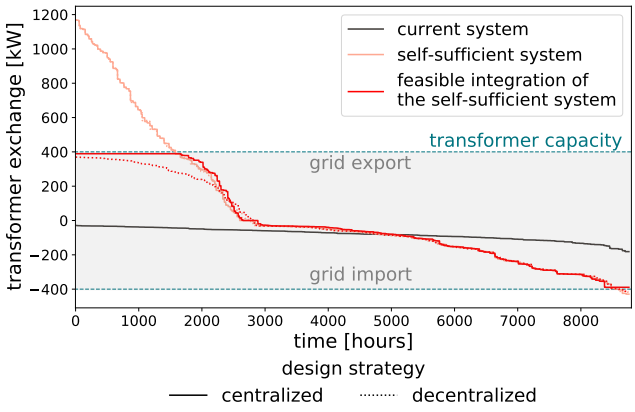

Fig. 8: Load duration curve on the local low-voltage transformer. Comparison of three different system scenarios: the current system, the identified system, which would be self-sufficient with a grid round tip efficiency of 70% and the latter system with modifications to be feasible at the transformer.

the district, lied clearly within the feasibility range of the transformer. The current system is characterized by the usage of gas boilers, a few heat pumps, and PV penetration so low that generated electricity is mainly consumed within the district. The aim in coming years is to drastically increase the level of PV integration, as it has been identified to be key on the way towards carbon neutrality [24]. Recent studies have demonstrated that the medium voltage level of the grid cannot host a large amount of PV installations [2].

Hence, the previously identified self-sufficient system including grid-aware PV integration and a storage system with a round-trip efficiency of 70% is further analyzed here. With a peak feed-in of 1200 kW, the system exceeds the 400 kW capacity of the local transformer. A central grid constraint limiting the exchange to a maximum of 400 kW was imposed while maintaining the PV panel integration. This analysis provided feasible results using the centralized design strategy, as shown in Figure 8; however, this central constraint cannot be imposed using the decentralized design strategy. Therefore, the grid usage limit was split according to the magnitude of the uncontrollable load of the buildings (Equation 10b). This procedure did lead to feasible solutions on the transformer but over-constrainted the system. Imposing the transformer limits allowed feasible integration of PV, but came with certain costs, which are further detailed in Figure 9.

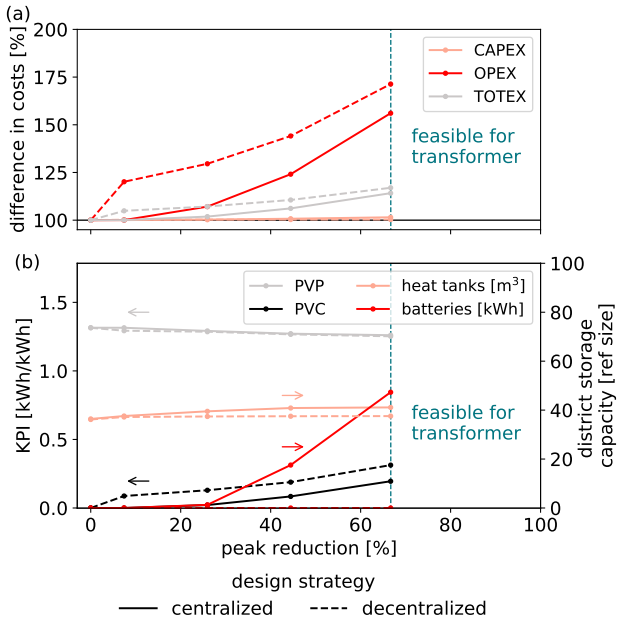

Fig. 9: Peak reduction for decentralized and centralized design strategy. a) Impact on related costs of the system and b) resulting PVC, PVP and storage system installations.

Peak reduction techniques are compared in Figure 9. The cost–optimal solution for the decentralized design strategy was to curtail excess electricity. More than 25% of PV electricity was curtailed, which decreased the PVP by 4% and increased the OPEX by 70% at current feed-in tariffs of 8 ct/kWh. Using the centralized design strategy, however, allowed the peak exchange to be reduced by 25% by strategically operating the district, without requiring additional PVC or storage units. In this case, the capacity of the thermal tanks was marginally increased. The remaining reduction was achieved by a coordinated operation of the heat pumps, preheating the buildings, and using west-facing facades instead of south-facing facades as the preferred choice for PV panel installations. However, PV curtailment was still required, as this was not enough to be feasible at the transformer. However, the most cost-effective solution was not to curtail the excess completely, but purchase a central battery for peak shaving. This purchase increased the overall CAPEX of the energy system by less than 1%.

The baseline system is the already analyzed system, considering the current building stock with a high level of electrification. Additionally to this baseline scenario, the need of PV panels to become self-sufficient was analyzed for different district scenarios. The identified energy systems that are required to meet SS with a round-trip efficiency of 70% all exceeded the capacity of the transformer. Given that the curtailed electricity cannot be sold at feed-in price to the grid, the OPEX increased (Figure 10).

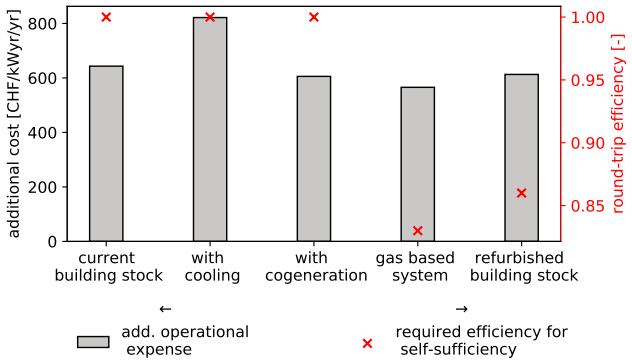

Fig. 10: Options for overcoming limitations imposed by the local transformer discussed in terms of increased operation costs and needed round-trip efficiency to remain self-sufficient.

The PVC was the most economic solution. However, once the PV panels are purchased, curtailing the electricity or using it within the district has the same outcome. For example, the electricity can be used to power already installed heat pumps in reverse mode to supply cooling demand in summer. As cooling must also be supplied during hours that are feasible at the transformer, the cost increase of this solution compared to the baseline scenario, without cooling is 800 CHF/kWyr/yr instead of 600 CHF/kWyr/yr of capacity shortage at the transformer. This is a benchmark price for the reinforcements of the system or for additional investments, which make a better use of the curtailed electricity. As electricity was curtailed in all analyzed systems, the round-tip efficiency needed to be increased to allow the system to remain self-sufficient. The baseline scenario required an ideal storage system to reach

SS, whereas refurbishing the building stock led to a more realistic required round-trip efficiency of 85%.

IV. Conclusion

The aim of this paper was to demonstrate the benefit of community-based design for distributed renewable energy hubs at the district scale. This centralized strategy is in contrast to the decentralized strategy which focuses on the optimal design and operation of a collection of buildings scale hubs. The Dantzig–Wolfe decomposition method was applied to the compact MILP formulation to access the centralized optimal solutions in a feasible computational time. The proposed centralized design strategy was applied to a MOO framework of a typical central European residential district in Switzerland; the results were then compared with those obtained using a decentralized strategy, which focuses on the optimal design and operation of single buildings. The main findings are listed below and were discussed in terms of 1) objective value, 2) PV penetration and 3) grid-aware integration of PV units.

1) The centralized optimization led to non-dominated solutions on the Pareto frontier and outperformed the decentralized strategy in each scenario. The improvement was especially apparent in low-investment scenarios.
2) With the centralized, coordinated investment and operation strategy, PV panel installations were economically feasible for a wide range of tariffs, starting as low as 3/10 ct/kWh to 0/12.5 ct/kWh for feed-in and demand price, respectively. In general the integration of renewable energy technologies at the district scale was enhanced compared to the decentralized strategy.
3) The centralization of the optimization allowed a grid-aware integration of renewable energy units. The coordinated operation, the adaptation of the PV orientations and the battery investments minimized the necessary PV curtailment to respect the local low-voltage transformer capacity.

The methodology contributed to the state-of-the art in district energy modeling, as entire low-voltage grids can be considered in a deterministic approach. Furthermore, the centralized strategy allowed for the consideration of centralized as well as distributed energy units and constraints in the renewable energy hub. A possible expansion of this work is to integrate seasonal storage systems or district heating and cooling network, which enable the inclusion of centralized cogeneration units and thermal energy exchange between buildings.

References

[1] O. Lucon and et. al, "Buildings," in *Climate Change 2014: Mitigation of Climate Change. Contribution of Working Group III to the Fifth Assessment Report of the Intergovernmental Panel on Climate Change*. United Kingdom and New York: Cambridge University Press, 2014.

[2] R. Gupta, F. Sossan, and M. Paolone, "Countrywide PV hosting capacity and energy storage requirements for distribution networks: The case of Switzerland," *Applied Energy*, vol. 281, p. 116010, Jan. 2021. [Online]. Available: https://linkinghub.elsevier.com/retrieve/pii/S0306261920314537

[3] M. Mohammadi, Y. Noorollahi, B. Mohammadi-ivatloo, M. Hosseinzadeh, H. Yousefi, and S. T. Khorasani, "Optimal management of energy hubs and smart energy hubs – A review," *Renewable and Sustainable Energy Reviews*, vol. 89, pp. 33–50, Jun. 2018. [Online]. Available: https://linkinghub.elsevier.com/retrieve/pii/S1364032118300601

[4] A. Maroufmashat, A. Elkamel, M. Fowler, S. Sattari, R. Roshandel, A. Hajimiragha, S. Walker, and E. Entchev, "Modeling and optimization of a network of energy hubs to improve economic and emission considerations," *Energy*, vol. 93, pp. 2546–2558, Dec. 2015. [Online]. Available: https://linkinghub.elsevier.com/retrieve/pii/S0360544215014474

[5] P. Stadler, L. Girardin, A. Ashouri, and F. Maréchal, "Contribution of Model Predictive Control in the Integration of Renewable Energy Sources within the Built Environment," *Frontiers in Energy Research*, vol. 6, May 2018. [Online]. Available: http://journal.frontiersin.org/article/10.3389/fenrg.2018.00022/full

[6] F. Belfiore, "District heating and cooling systems to integrate renewable energy in urban areas," Ph.D. dissertation, 2021, publisher: Lausanne, EPFL. [Online]. Available: http://infoscience.epfl.ch/record/289467

[7] B. Morvaj, R. Evins, and J. Carmeliet, "Optimization framework for distributed energy systems with integrated electrical grid constraints," *Applied Energy*, vol. 171, pp. 296–313, Jun. 2016. [Online]. Available: https://linkinghub.elsevier.com/retrieve/pii/S0306261916304159

[8] A. Fakhri, M. Ghatee, A. Fragkogios, and G. K. Saharidis, "Benders decomposition with integer subproblem," *Expert Systems with Applications*, vol. 89, pp. 20–30, Dec. 2017. [Online]. Available: https://linkinghub.elsevier.com/retrieve/pii/S0957417417304864

[9] C. Chen, B. He, Y. Ye, and X. Yuan, "The direct extension of ADMM for multi-block convex minimization problems is not necessarily convergent," *Mathematical Programming*, vol. 155, no. 1-2, pp. 57–79, Jan. 2016. [Online]. Available: http://link.springer.com/10.1007/s10107-014-0826-5

[10] L. Sokoler, L. Standardi, K. Edlund, N. Poulsen, H. Madsen, and J. Jørgensen, "A Dantzig–Wolfe decomposition algorithm for linear economic model predictive control of dynamically decoupled subsystems," *Journal of Process Control*, vol. 24, no. 8, pp. 1225–1236, Aug. 2014. [Online]. Available: https://linkinghub.elsevier.com/retrieve/pii/S0959152414001504

[11] I. E. Grossmann, "Advances in mathematical programming models for enterprise-wide optimization," *Computers & Chemical Engineering*, vol. 47, pp. 2–18, Dec. 2012. [Online]. Available: https://linkinghub.elsevier.com/retrieve/pii/S0098135412002220

[12] J. R. Tebboth, "A computational study of Dantzig-Wolfe decomposition," Ph.D. dissertation, University of Buckingham, 2001.

[13] G. Rius-Sorolla, J. Maheut, S. Estellés-Miguel, and J. P. Garcia-Sabater, "Coordination mechanisms with mathematical programming models for decentralized decision-making: a literature review," *Central European Journal of Operations Research*, vol. 28, no. 1, pp. 61–104, Mar. 2020. [Online]. Available: http://link.springer.com/10.1007/s10100-018-0594-z

[14] T. H. Summers and J. Lygeros, "Distributed model predictive consensus via the Alternating Direction Method of Multipliers," in *2012 50th Annual Allerton Conference on Communication, Control, and Computing (Allerton)*. Monticello, IL, USA: IEEE, Oct. 2012, pp. 79–84. [Online]. Available: http://ieeexplore.ieee.org/document/6483202/

[15] T. Schütz, X. Hu, M. Fuchs, and D. Müller, "Optimal design of decentralized energy conversion systems for smart microgrids using decomposition methods," *Energy*, vol. 156, pp. 250–263, Aug. 2018. [Online]. Available: https://linkinghub.elsevier.com/retrieve/pii/S0360544218308703

[16] H. Harb, J.-N. Paprott, P. Matthes, T. Schütz, R. Streblow, and D. Müller, "Decentralized scheduling strategy of heating systems for balancing the residual load," *Building and Environment*, vol. 86, pp. 132–140, Apr. 2015. [Online]. Available: https://linkinghub.elsevier.com/retrieve/pii/S0360132314004260

[17] Y. Yang, S. Zhang, and Y. Xiao, "Optimal design of distributed energy resource systems coupled with energy distribution networks," *Energy*, vol. 85, pp. 433–448, Jun. 2015. [Online]. Available: https://linkinghub.elsevier.com/retrieve/pii/S0360544215004107

[18] T. Wakui, M. Hashiguchi, and R. Yokoyama, "Structural design of distributed energy networks by a hierarchical combination of variable- and constraint-based decomposition methods," *Energy*, vol. 224, p. 120099, Jun. 2021. [Online]. Available: https://linkinghub.elsevier.com/retrieve/pii/S0360544221003480

[19] L. Middelhauve, L. Girardin, F. Baldi, and F. Maréchal, "Potential of Photovoltaic Panels on Building Envelopes for Decentralized District Energy Systems," *Frontiers in Energy Research*, vol. 9, pp. 689–781, Oct. 2021. [Online]. Available: https://www.frontiersin.org/articles/10.3389/fenrg.2021.689781/full

[20] L. Middelhauve, F. Baldi, P. Stadler, and F. Maréchal, "Grid-Aware Layout of Photovoltaic Panels in Sustainable Building Energy Systems," *Frontiers in Energy Research*, vol. 8, p. 573290, Feb. 2021. [Online]. Available: https://www.frontiersin.org/articles/10.3389/fenrg.2020.573290/full

[21] P. M. Stadler, "Model-based sizing of building energy systems with renewable sources," Ph.D. dissertation, EPFL, 2019. [Online]. Available: http://infoscience.epfl.ch/record/267499/files/EPFL_TH9560.pdf

[22] J. Holweger, L. Bloch, C. Ballif, and N. Wyrsch, "Mitigating the impact of distributed PV in a low-voltage grid using electricity tariffs," *arXiv:1910.09807 [cs, eess]*, Oct. 2019, arXiv: 1910.09807. [Online]. Available: http://arxiv.org/abs/1910.09807

[23] L. Middelhauve, A. Santecchia, L. Girardin, and F. Marechal, "Key Performance Indicators for Decision Making in Building Energy Systems," in *Proceedings of ECOS 2020*, Jun. 2020.

[24] R. Nordmann, *Sonne für den Klimaschutz: ein Solarplan für die Schweiz*, 1st ed. Basel: Zytglogge, 2019.